УДК 537.591

АТМОСФЕРНЫЕ МЮОНЫ ПРИ ОЧЕНЬ ВЫСОКИХ ЭНЕРГИЯХ

[1]А.А. Кочанов, [2]Т.С. Синеговская, [1]С.И. Синеговский,
[3]А. Мисаки, [4]Н. Такахаши

ATMOSPHERIC MUONS AT VERY HIGH ENERGIES

[1]AA. Kochanov, [2]T.S Sinegovskaya, [1]S.I. Sinegovsky,
[3]A. Misaki, [4]N. Takahashi

В ближайшем будущем станет реально измеримым на детекторах объемом в кубический километр спектр атмосферных мюонов при энергиях свыше нескольких сотен ТэВ. Ожидается, что эти измерения позволят существенно уменьшить неопределенности потока мюонов при энергиях выше 50 ТэВ, обусловленные слабоизученными процессами рождения очарованных частиц и большими ошибками в измерениях спектра и состава первичных космических лучей. Мы приводим результаты расчета вертикального спектра мюонов на уровне моря, выполненного для трех моделей взаимодействия адронов при очень высоких энергиях с учетом вклада в потоки мюонов распада очарованных частиц.

In the near future the energy region above few hundreds of TeV may really be accessible to measure the atmospheric muon spectrum by cubic kilometre detectors. One expects that muon flux uncertainties above 50 TeV, related to a poor knowledge of charm production cross sections and insufficiently examined primary spectra and composition, will be diminished. We give predictions for the very high-energy cosmic ray muon spectrum at sea level, obtained with the three hadronic interaction models, taking into consideration also the muon contribution due to decays of the charmed particles.

Introduction

The atmospheric neutrino flux at high energies is inevitably dominated by the prompt component due to decays of the charmed hadrons ($D^{\pm}$, D^{0}, $\bar{D}^{0}$, $D_s^{\pm}$, Λ_c^{+}), hence the prompt neutrino flux becomes the major source of the background in searches for a diffuse astrophysical neutrino flux [1–4]. Insufficiently explored processes of charm production give rise to most uncertainty in muon and neutrino fluxes. IceCube, the first to begin operating as the Km3 neutrino telescope, has the real capability [5] to measure the atmospheric muon spectrum at energies up to 1 PeV and to shed light on the feasible range of cross sections for charmed particle production.

In this work, we try to extend the muon flux calculations to higher energies based on the active hadronic interaction models using the most reliable data from primary cosmic ray measurements. We present results of conventional muon flux calculations in the range of $10–10^7$ GeV using hadronic models QGSJET-II 03 [6, 7], SIBYLL 2.1 [8, 9], EPOS [10–12] as well as Kimel and Mokhov (KM) [13] that were also tested in recent atmospheric muon flux calculations [14, 15]. At the muon energies $E \gtrsim 50$ TeV, we add the prompt muon flux originating from decays of charmed hadrons produced in collisions of cosmic rays with nuclei of air (for review see e.g. [16–19]).

The method

High-energy muon fluxes are calculated using the approach [20] to solve the atmospheric hadron cascade equations, taking into account the non-scaling behavior of inclusive particle production cross-sections, rise in total inelastic hadron-nuclei cross-sections, and non-power law primary spectrum (see also [15]).

To obtain the differential energy spectra of protons $p(E, h)$ and neutrons $n(E, h)$ at the depth h one needs to solve the set of equations:

$$\frac{\partial N^{\pm}(E,h)}{\partial h} = \frac{N^{\pm}(E,h)}{\lambda_N(E)} + \frac{1}{\lambda_N(E)} \int_0^1 \Phi_{NN}^{\pm}(E,x) N^{\pm}(E/x,h) \frac{dx}{x^2}, \quad (1)$$

where $N^{\pm}(E,h) = p(E,h) \pm n(E,h)$,

$$\Phi_{NN}^{\pm}(E,x) = \frac{E}{\sigma_{pA}^{in}(E)} \left[\frac{d\sigma_{pp}(E_0,E)}{dE} \pm \frac{d\sigma_{pn}(E_0,E)}{dE} \right],$$

$\lambda_N(E) = 1/\left[N_0 \sigma_{pA}^{in}(E) \right]$ is the nucleon interaction length; $x=E/E_0$ is the fraction of energy carried away by the secondary nucleon; E_0 and E – energies of the projectile and final nucleons $d\sigma_{ab}/dE$ – differential cross sections for inclusive reaction $a+A \to b+X$. The boundary conditions for Eq. (1) are $N^{\pm}(E, 0)=p_0(E)n_0(E)$.

Consider that the solution of the system is

$$N^{\pm}(E,h) = N^{\pm}(E,0) \exp\left[-\frac{h\left(1 - Z_{NN}^{\pm}(E,h)\right)}{\lambda_N(E)} \right], \quad (2)$$

where $Z_{NN}^{\pm}(E,h)$ are unknown functions. Substituting Eq. (2) into Eq. (1), we find the equation for these functions $Z_{NN}^{\pm}(E,h)$ (Z-factors):

$$\frac{\partial (h Z_{NN}^{\pm})}{\partial h} = \int_0^1 \Phi_{NN}^{\pm}(E,x) \eta_{NN}^{\pm}(E,x) \exp\left[-h D_{NN}^{\pm}(E,x,h) \right] dx, \quad (3)$$

where $\eta_{NN}^{\pm}(E,x) = x^{-2} N^{\pm}(E/x, 0) / N^{\pm}(E, 0)$,

$$D_{NN}^{\pm}(E,x,h) = \frac{1 - Z_{NN}^{\pm}(E/x,h)}{\lambda_N(E/x)} - \frac{1 - Z_{NN}^{\pm}(E,h)}{\lambda_N(E)}.$$

By integrating Eq. (3) we obtain the nonlinear integral equation

$$Z^{\pm}_{NN}(E,h)=\frac{1}{h}\int_0^h dt\int_0^1 \Phi^{\pm}_{NN}(E,x)\eta^{\pm}_{NN}(E,x)\times,$$
$$\times\exp\left[-tD^{\pm}_{NN}(E,x,t)\right]dx \qquad (4)$$

which can be solved by iterations. The simple choice of zero-order approximation is $Z^{\pm(0)}_{NN}(E,h)=0$, that is $D^{\pm(0)}_{NN}(E,x,h)=\frac{1}{\lambda_N(E/x)}-\frac{1}{\lambda_N(E)}$. For the n-th step we find

$$Z^{\pm(n)}_{NN}(E,h)=\frac{1}{h}\int_0^h dt\int_0^1 \Phi^{\pm}_{NN}(E,x)\eta^{\pm}_{NN}(E,x)\times$$
$$\times\exp\left[-tD^{\pm(n-1)}_{NN}(E,x,t)\right]dx, \qquad (5)$$

$$D^{\pm(n)}_{NN}(E,x,h)=\frac{1-Z^{\pm(n)}_{NN}(E/x,h)}{\lambda_N(E/x)}-\frac{1-Z^{\pm(n)}_{NN}(E,h)}{\lambda_N(E)}. \qquad (6)$$

Nontrivial structure of the nucleon Z-factors (Fig. 1) results from the non-power law behavior of the ATIC-2 primary spectrum (see later), non-scaling behavior of particle production cross-sections and energy dependence of inelastic hadron-nucleus cross-sections. After that, using the obtained nucleon fluxes, we are able to calculate successively the meson and the lepton fluxes [15].

In our calculations we rely on recent data on primary cosmic ray (PCR) spectra and composition obtained with Advanced Thin Ionization Calorimeter, balloon-borne experiment ATIC-2 [21]. In order to extend the calculations to higher energies, up to 10 PeV, we use data from the GAMMA experiment [22]. The energy spectra and elemental composition obtained in the GAMMA experiment cover the 10^3–10^5 TeV range and agree with the corresponding extrapolations of the known balloon and satellite data at $E\geq10^3$ TeV. Alternative primary spectrum used in the calculations for a region of very high energies is the model by Zatsepin and Sokolskaya (ZS) [23, 24]. The ZS proton spectrum at $E\geq10^6$ GeV is compatible with KASCADE data [25, 26] and the helium one is within the range of the KASCADE spectrum reconstructed using QGSJET 01 and SIBYLL models. Besides we apply the Gaisser and Honda spectra (GH) [27, 28] to compute the muon flux in more narrow energy range $E\square10^5$ GeV.

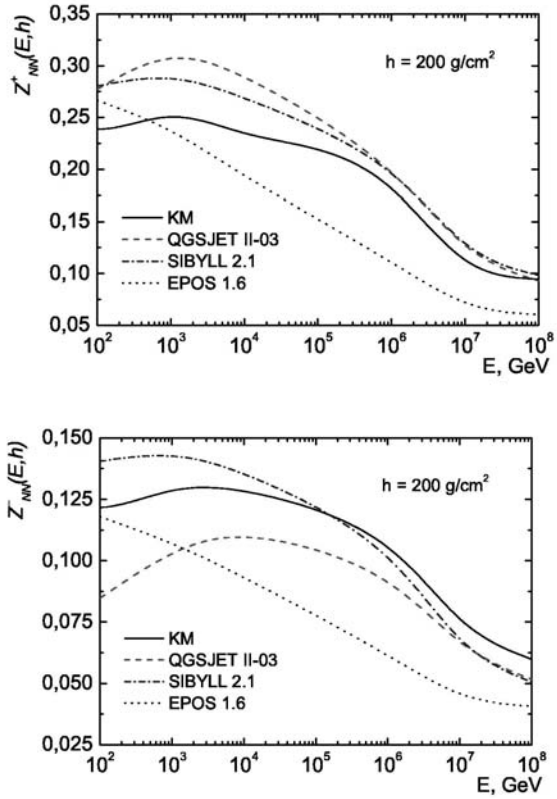

Fig. 1. The energy dependence of $Z^{\pm}_{NN}(E,h)$ – factors at the depth of 200 gcм$^{-2}$ calculated for the ATIC-2 primary spectrum.

High-energy muon spectra

Apart from evident sources of AM, $\pi_{\mu2}$ and $K\mu_2$ decays, we take into consideration three-particle semileptonic decays, $K^{\pm}_{\mu3}$, $K^{0}_{\mu3}$, and a small fraction of the muon flux resulted from decay chains $K\to\pi\to\mu$ ($K^0_S\to\pi^+ +\pi^-$, $K^{\pm}\to\pi^{\pm}+\pi^0$).

The prompt muon contribution due to decays of charmed hadrons at high energies is considered for the three charm production models: the recombination quark-parton model (RQPM) [16], quark-gluon string model QGSM [16, 17, 29–32], and the model by Pasquali, Reno and Sarcevic (PRS) [33] (see also [19]). Both RQPM and QGSM are nonperturbative models, whereas PRS is based on the next-to-leading-order QCD calculations.

The high-energy spectra of conventional and prompt muons at ground level calculated for the vertical direction are shown in Fig. 2 along with experimental data. The shaded areas here indicate the calculations of the conventional muon flux with KM model for the case of the ATIC-2 primary spectrum (light band on the left) and the GAMMA one (dark band on the right). The size of the bands corresponds to statistical errors in the ATIC-2

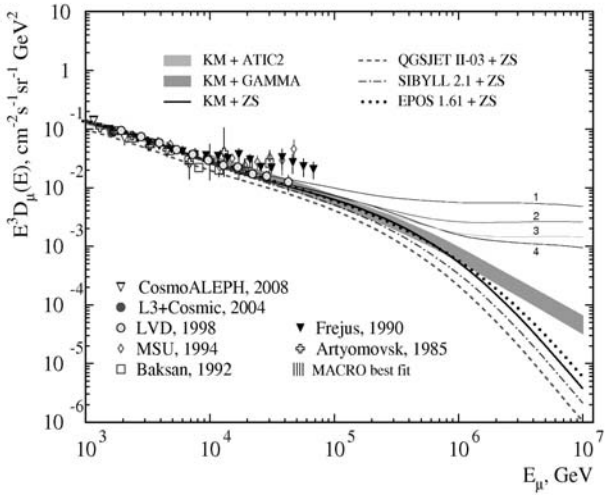

Fig. 2. The high energy vertical muon spectra at ground level. The dashed-line curves and shaded areas present this work calculations with the ATIC-2 primary spectrum [21] (E_μ<10 TeV) and GAMMA one (E_μ<10 TeV). The solid curve marks the computation for the primary spectrum model by Zatsepin and Sokolskaya [23, 24]. The numbers near thin lines indicate the prompt muon flux model: 1 – RQPM [16], 2 and 3 – two calculation versions of PRS [33], 4 – QGSM [16, 17].

and GAMMA experiments. Solid, dashed, dash-dotted, and dotted lines indicate the calculations with the ZS spectrum and set of hadronic models, KM, SIBYLL 2.1EPOS 1.61, and QGSJET-II. The experimental data comprise the measurements of L3+Cosmic [34], Cosmo-ALEPH [35, 36] as well as the data (converted to the surface) of deep underground experiments MSU [37], MACRO [38], LVD [39], Frejus [40], Baksan [41], Artyomovsk [42]. Notice that the calculation results do not fit well the Frejus and MSU data even though taking into account the prompt muon component (thin lines in Fig. 2), while the LVD data are described well.

The ZS model seems to be a reasonable bridge from TeV energy range to PeV one, providing a junction of the different energy ranges. Above 10^6 GeV, the muon flux is apparently affected by the primary cosmic ray ambiguity in the vicinity of `knee'.

Muon charge ratio

The muon charge ratio depends on the proton to neutron ratio in primary cosmic rays as well as on the hadron production cross-sections. Thus, the comparison of the calculated μ^+/μ^- ratio with experimental data in a wide energy range allows these features to be studied indirectly. At present, the muon charge ratio is measured with new facilities providing high quality data from a large number of muon events at high energies.

In Fig. 3, we present our calculations of μ^+/μ^- ratio along with the data from experiments [34–36, 43–52]. The calculations are made with the three hadronic interaction models and two primary cosmic ray spectra. Solid and dashed lines mark the KM + GH computation for the zenith angles 0°and 90°, thin line indicates the KM + ZS result at 0°. Bold dotted line indicates the SIBYLL 2.1 + GH result, dotted shows the QGSJET-II + GH one, both for 0°. One may see that the KM and SIBYLL calculations reproduce data well with both versions of the primary spectra, GH and ZS. The calculated curves correspond approximately to the value 1.3 that is in agreement with the recent data from BESS–TeV,

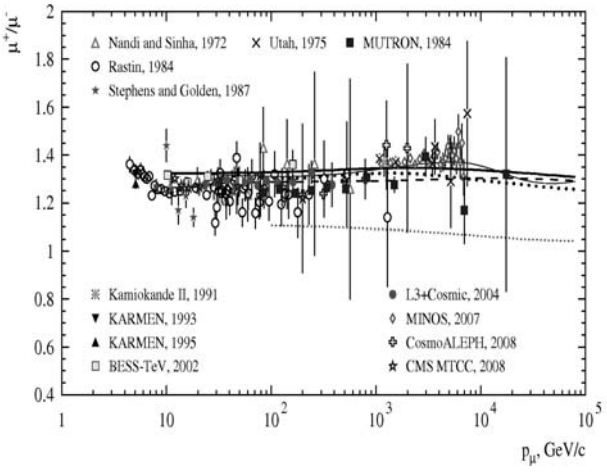

Fig. 3. Muon charge ratio at ground level computed for the three hadronic interaction models and the two primary cosmic ray spectra. Solid line marks the KM + GH result for θ=0°, dashed line shows the same at θ=90°. Thin line: the KM + ZS at 0°, bold-dotted: the SIBYLL 2.1 + GH, dotted (the lower): QGSJET-II + GH at 0°.

CosmoALEPH, and L3+Cosmic experiments up to 1 TeV. For higher energies, the kaon source of muons becomes more intensive leading to a maximum of the muon ratio, ~1.4, at energy close to 10 TeV. This value agrees with the recent results of the MINOS far detector [50]. The calculations are also in agreement with the spectrograph MUTRON data [46] at θ=89°, including the point above 10 TeV.

The QGSJET-II model (lower line) shows an apparent the deviation from others: the predicted μ^+/μ^- ratio is close to ~1.2 that might be explained by the higher extent of the proton and neutron flux equalization in the atmosphere due to reactions $pA \rightarrow nX$ in the model (see Fig. 1).

Conclusions

One may expect that the primary cosmic ray uncertainty beyond the `knee' would be negligible, if real prompt muons at energies around ~10^6 GeV (Fig. 2) would appear at the flux level that is not much lower than the QGSM prediction.

It seems reasonable to consider that the prompt muon flux higher than it is predicted by RQPM is excluded [3]. One may expect that stronger restrictions of the prompt muon flux range will be extracted from the experiment in the near future.

We are grateful to T. Pierog for clarifying comments concerning codes of the hadronic interaction models. This research was partly supported by the Russian Federation Ministry of Education and Science within the Program «Development of Scientific Potential in Higher Schools» under grants 2.2.1.1/1483, 2.1.1/1539, «Scientific and educational cadres for innovation Russia», grant P1242, and by Federal Program «Russian Scientific Schools», grant NSh-1027.2008.2.

REFERENCES

1. Aynutdinov V. et al. Search for a diffuse flux of high-energy extraterrestrial neutrinos with the NT200 neutrino telescope // Astropart. Phys. 2006. V. 25. P. 140.

2. Aynutdinov V. et al. The Baikal neutrino experiment: Status, selected physics results, and perspectives // Nucl. Instrum. Meth. A 2008.V. 588. P. 99.

3. Achterberg A. et al. (IceCube Collaboration) Multiyear search for a diffuse flux of muon neutrinos with AMANDA-II // Phys. Rev. D. 2007. V. 76, 042008.

4. Ackermann M. et al. Search for Ultra-High-Energy Neutrinos with AMANDA-II // ApJ. 2008. V. 675. P. 1014.

5. Berghaus P. for the IceCube Collaboration. Muons in IceCube, arXiv:0902.0021v1 [astro-ph].

6. Ostapchenko S.S. QGSJET-II: towards reliable description of very high energy hadronic interactions // Nucl. Phys. B (Proc. Suppl.). 2006. V. 151. P. 143.

7. Ostapchenko S. Nonlinear screening effects in high energy hadronic interactions // Phys. Rev. D. 2006. V. 74. P. 014026.

8. Fletcher R.S. et al. SIBYLL: An event generator for simulation of high energy cosmic ray cascades // Phys. Rev. D. 1994. V. 50. P. 5710.

9. Engel R. et al. Air Shower Calculations With the New Version of SIBYLL // Proc. 26th ICRC, Salt Lake City, 1999. V. 1. P. 415.

10. Werner K., Pierog T. Extended Air Shower Simulations Based on EPOS // AIP Conf. Proc. 2007. V. 928. P. 111. astro-ph/0707.3330.

11. Pierog T., Werner K. Hadronic Interaction Model EPOS and Air Shower Simulations: New Results on Muon Production // Proc. 30th ICRC, Merida, 2007. HE.1.6, N. 905.

12. Werner K. The hadronic interaction model EPOS // Nucl. Phys. B (Proc. Suppl.). 2008. V. 175–176. P. 81.

13. Kalinovsky A.N., Mokhov N.V., Nikitin Yu. P. Passage of high-energy particles through matter, AIP, New York, 1989.

14. Kochanov A.A. et al. Calculation of the atmospheric muon flux motivated by the ATIC-2 experiment // Proc. 30th ICRC, Universidad Nacional Auto'noma de Me'xico, Mexico City, Mexico, 2008. V. 5. P. 1511. astro-ph/0706.4389.

15. Kochanov A.A., Sinegovskaya T.S., Sinegovsky S.I. High-energy cosmic-ray fluxes in the Earth atmosphere: Calculations vs experiments // Astropart. Phys. 2008. V. 30. P. 219. axXiv:0803.2943v2 [astro-ph].

16. Bugaev E.V. et al. On the interpretation of the Kamiokande neutrino experiment // Nuovo Cim. C. 1989. V. 12. P. 41.

17. Bugaev E.V. et al. Atmospheric muon flux at sea level, underground, and underwater // Phys. Rev. D. 1998. V. 58. P. 054001.

18. Misaki A. et al. Fluxes of atmospheric muons underwater depending on the small-x gluon density // J. Phys. G. 2003. V. 29. P. 387.

19. Enberg R., Reno M.H., Sarcevic I. Prompt neutrino fluxes from atmospheric charm // Phys. Rev. D 2008. V. 78. P. 043005.

20. Naumov V.A., Sinegovskaya T.S. Simple method for solving transport equations describing the propagation of cosmic-ray nucleons in the atmosphere // Phys. Atom. Nucl. 2000. V. 63. P. 1927.

21. Panov A.D. et al. Elemental energy spectra of cosmic rays from the data of the ATIC-2 experiment // Bull. Russ. Acad. Sci. Phys. 2007. V. 71. P. 494. astro-ph/0612377.

22. Garyaka A.P. et al. Rigidity-dependent cosmic ray energy spectra in the knee region obtained with the GAMMA experiment // Astropart. Phys. 2007. V. 28. P. 169.

23. Zatsepin V.I., Sokolskaya N.V. Three component model of cosmic ray spectra from 10 GeV to 100 PeV // Astron. Astrophys. 2006. V. 458. P. 1.

24. Zatsepin V.I., Sokolskaya N.V. Energy spectra of the main groups of galactic cosmic rays in the model of three classes of sources // Astron. Lett. 2007. V. 33, N. 1. P. 25.

25. Antoni T. et al. KASCADE measurements of energy spectra for elemental groups of cosmic rays: Results and open problems // Astropart. Phys. 2005. V. 24. P. 1.

26. Apel W.D. et al. Energy spectra of elemental groups of cosmic rays: Update on the KASCADE unfolding analysis // Astropart. Phys. 2009. V. 31. P. 86.

27. Gaisser T.K. et al. Primary spectrum to 1 TeV and beyond // Proc. 27th ICRC, Hamburg, 2001. V. 1. P. 1643.

28. Gaisser T.K., Honda M. Flux of atmospheric neutrinos // Annu. Rev. Nucl. Part. Sci. 2002. V. 52. P. 153.

29. Kaidalov A.B., Piskunova O.I. // Sov. J. Nucl. Phys. 1985. V. 41. P. 816.

30. Kaidalov A.B., Piskunova O.I. Production of charmed particles in the quark-gluon string model // Sov. J. Nucl. Phys. 1986. V. 43. P. 994.

31. Kaidalov A.B., Piskunova O.I. Inclusive spectra of baryons in the quark-gluon strings model // Z. Phys. C. 1986. V. 30. P. 145.

32. Piskunova O.I. Inclusive distributions and cross-sections for hadroproduction of heavy flavored particles in the quark-gluon string model // Sov. J. Nucl. Phys. 1993. V. 56. P. 1094.

33. Pasquali L., Reno M.H., Sarcevic I. Lepton fluxes from atmospheric charm // Phys. Rev. D. 1999. V. 59. P. 034020.

34. Achard P. et al. Measurement of the atmospheric muon spectrum from 20 to 3000 GeV // Phys. Lett. B. 2004. V. 598. P. 15.

35. Grupen C. Cosmic Ray Results from the CosmoALEPH Experiment // Nucl. Phys. B (Proc. Suppl.). 2008. V. 175–176. P. 286.

36. Omar Hashim N. Measurement of the momentum spectrum of cosmic ray muons at a depth of 320 mwe // CERN-THESIS-2007-047.

37. Zatsepin G.T. et al. Energy spectrum of PCR nucleons in the range 20-TeV to 400-TeV and charm generation from the muon experiment of Lomonosov State University // Izv. Ross. Akad. Nauk. Fiz. 1994. V.58. P. 119.

38. Ambrosio M. et al. Vertical muon intensity measured with MACRO at the Gran Sasso Laboratory // Phys. Rev. D. 1995. V. 52. P. 3793.

39. Aglietta M. et al. Muon "Depth intensity" relation measured by LVD underground experiment and cosmic ray muon spectrum at sea level // Phys. Rev. D. 1998. V. 58. P. 092005.

40. Rhode W. Measurements of the muon flux with the Fréjus-detector // Nucl. Phys. B (Proc. Suppl.). 1994. V. 35. P. 250.

41. Bakatanov V.N. et al. Intensity of cosmic ray muons and of primary nucleons according to data from the Baksan underground scintillation telescope // Yad. Fiz. 1992. V. 55. P. 2107.

42. Enikeev R.I. et al. Study of muon spectrum at the depth of 570 m.w.e. underground with 100-ton scintillation detector// Yad. Fiz. 1988. V. 47. P. 1044.

43. Haino S. et al. Measurements of primary and atmospheric cosmic-ray spectra with the BESS-TeV spectrometer // Phys. Lett. B. 2004. V. 594. P. 35.

44. Nandi B.C., Sinha M.S., The momentum spectrum of muons at sea level in the range 5-1200 Gev/c // J. Phys. A. 1972. V. 5. P. 1384.

45. Ashley G.K., Keuffel J.W., Larson M.O. Charge ratio of ultra-high-energy cosmic-ray muons // Phys. Rev. D. 1975. V. 12. P. 20.

46. Matsuno S. et al. Cosmic ray muon spectrum up to 20 TeV at 89º zenith angle // Phys. Rev. D. 1984. V. 29. P. 1.

47. Rastin B.C. A study of the muon charge ratio at sea level within the momentum range 4 GeV/c to 2000 GeV/c // J. Phys. G. 1984. V. 10. P. 1629.

48. Stephens S.A., Golden R.L. // Proc. 20th ICRC, Moscow, 1987. V. 6. P. 173.

49. Jannakos T.E. Muon capture reactions on C-12 and C-13 in the KARMEN detector // FZKA Report 5520, 1995.

50. Adamson P. et al. Measurement of the atmospheric muon charge ratio at TeV energies with the MINOS detector // Phys. Rev. D. 2007. V. 76. P. 052003.

51. Yamada M. et al. Measurements of the charge ratio and polarization of 1.2-TeV/c cosmic-ray muons with the Kamiokande II detector // Phys. Rev. D. 1991. V. 44. P. 617.

52. Aldaya M., Garcia-Abia P. Measurement of the charge ratio of cosmic muons using CMS data // CMS NOTE-2008/016, CERN Document Server: http://cdsweb.cern.ch

[1]*Иркутский государственный университет, Иркутск*
[2]*Иркутский государственный университет путей сообщения, Иркутск*
[3]*Research Institute for Science and Engineering, Waseda U., Tokyo, Japan*
[4]*Graduate School of Science and Technology, Hirosaki U., Hirosaki, Japan*